Spin and the Honeycomb Lattice: Lessons from Graphene

Matthew Mecklenburg[1,2] and B. C. Regan[1,2,*]

[1]Department of Physics and Astronomy, University of California, Los Angeles, California 90095, USA
[2]California NanoSystems Institute, University of California, Los Angeles, California 90095, USA

(Received 31 October 2010; published 16 March 2011)

A model of electrons hopping from atom to atom in graphene's honeycomb lattice gives low-energy electronic excitations that obey a relation formally identical to a 2 + 1 dimensional Dirac equation. Graphene's spin equivalent, "pseudospin," arises from the degeneracy introduced by the honeycomb lattice's two inequivalent atomic sites per unit cell. Previously it has been thought that the usual electron spin and the pseudospin indexing the graphene sublattice state are merely analogues. Here we show that the pseudospin is also a real angular momentum. This identification explains the suppression of electron backscattering in carbon nanotubes and the angular dependence of light absorption by graphene. Furthermore, it demonstrates that half-integer spin like that carried by the quarks and leptons can derive from hidden substructure, not of the particles themselves, but rather of the space in which these particles live.

DOI: 10.1103/PhysRevLett.106.116803 PACS numbers: 73.22.Pr, 03.65.Pm, 11.15.Ha, 71.10.Fd

"Spin" refers to an angular momentum that has no classical analogue—it is not possible to understand spin in terms of a mechanical model of some rotating object [1]. The net angular momentum of composite particles, such as protons, neutrons, atoms, and molecules, derives from the spins of their constituents, plus any orbital angular momenta due to the constituents' relative motion. Spin and orbital angular momenta are quantitatively distinguishable, since the former can be half-integer while the latter take on integer values only, measured in units of the reduced Planck constant $\hbar$. In the standard model of particle physics the ultimate constituents of matter are the quarks and leptons. These particles have no internal structure down to length scales of 10^{-18} m (limited by the collision energies ~200 GeV currently achievable in particle accelerators) [2], so their spins are considered intrinsic.

The deepest insight into the origin of spin has been provided by Dirac, who manipulated Einstein's quadratic energy-momentum relation $E^2 = p^2c^2 + m^2c^4$ to give a linear equation consistent with the postulates of quantum mechanics. Dirac's equation predicts not only spin but also antiparticles, which were unknown at the time. Thus we understand, for example, the electron's spin $\hbar/2$ and the existence of the positron as natural consequences of the Dirac equation, which is built on the theories of relativity and quantum mechanics. As was pointed out 25 years ago [3,4], the low-energy electronic excitations in graphene obey a 2 + 1 dimensional Dirac equation, with holes and the sublattice state playing the role of positrons and spin, respectively. In this Letter we show that the sublattice state vector describes an "intrinsic" angular momentum in 3 + 1 dimensions. This identification provides a physical model that associates spin with an underlying structure. Unlike the case of composite particles, where spin follows from other spins, in this example the spin $\hbar/2$ is a consequence of the nontrivial spatial lattice, invisible at low energies, that hosts the particle.

Graphene's Dirac equation follows from the tight-binding (i.e., hopping) model, which was first applied to graphene by Wallace [5]. With the experimental isolation of carbon nanotubes [6] and, more recently, graphene itself [7], the hopping model has been shown to give an effective description of these real materials [8,9]. Furthermore, graphene equivalents of the quantum relativistic effects implied by the Dirac equation, such as Klein tunneling and *Zitterbewegung*, are now experimentally accessible, making this condensed matter system a practical test bed for these particle physics phenomena [10,11].

We first show how the hopping model produces the 2 + 1 dimensional Dirac equation, working in 3 + 1 dimensions but without initial reference to specific coordinate axes. Graphene's electronic states are described as a linear combination [12] of atomic orbitals constructed to fulfill the Bloch condition $\Psi_{\mathbf{Q}}(\mathbf{r} + \mathbf{R}) = e^{i\mathbf{Q}\cdot\mathbf{R}}\Psi_{\mathbf{Q}}(\mathbf{r})$,

$$\Psi_{\mathbf{Q}}(\mathbf{r}) = \sum_{j}^{N} \frac{e^{i\mathbf{Q}\cdot\mathbf{R}_j}}{\sqrt{N}} [c^A_{\mathbf{Q}}\phi(\mathbf{r} - \mathbf{R}^A_j) + c^B_{\mathbf{Q}}\phi(\mathbf{r} - \mathbf{R}^B_j)], \quad (1)$$

where $j = (m, n)$ indexes the N sites of the hexagonal Bravais lattice described by $\mathbf{R}_j = m\mathbf{a}_1 + n\mathbf{a}_2$, and the vectors $\mathbf{R}^A_j$ ($\mathbf{R}^B_j$) point to the "A" ("B") sublattice sites within the unit cell j, respectively (see Fig. 1). Indices labeling the usual electron spin have been suppressed for notational convenience and will be henceforth. The coefficients $c_{\mathbf{Q}}$ multiplying the carbon atoms' $2P_z$ atomic orbitals $\phi(\mathbf{r})$ are chosen to solve the crystal Hamiltonian.

The electronic Hamiltonian contains two kinds of terms, one representing an electron's energy on a particular site, and the other representing the energy advantage conferred by the freedom to hop to a neighboring site. Nearest-neighbor hopping is parametrized by an energy t,

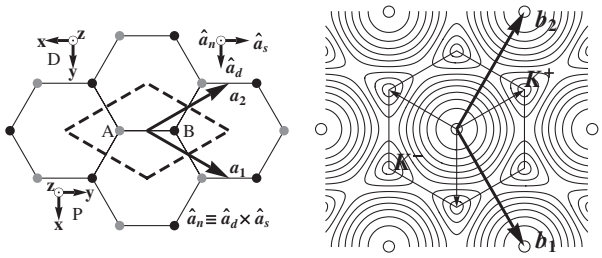

FIG. 1. The honeycomb lattice in real space (left) and the corresponding band structure in reciprocal space (right). On the left, gray and black circles represent A and B lattice sites, respectively. One choice of unit cell is demarcated with a dashed line. Coordinate axes oriented to give the Pauli and Dirac forms of the electronic Hamiltonian are labeled "P" and "D." On the right, the hexagonal first Brillouin zone is shown, with the positions of $\mathbf{K}^+$ points indicated by thin arrows. While generally the contours of constant energy [based on the full Hamiltonian (4)] show threefold or sixfold rotational symmetry, near the points $\mathbf{K}^\pm$ they are circular [8,12].

and next-nearest-neighbor and higher order effects are neglected. An electron occupying the state $\phi(\mathbf{r} - \mathbf{R}_j^A)$ is described by an operator $A^\dagger_{\mathbf{R}_j}$ that creates an electron on the "A" site in cell j when it acts on the vacuum state $|0\rangle$. With similar language for the "B" sites, the graphene Hamiltonian is

$$H = \sum_j (\mathcal{E}_A A^\dagger_{\mathbf{R}_j} A_{\mathbf{R}_j} + \mathcal{E}_B B^\dagger_{\mathbf{R}_j} B_{\mathbf{R}_j}) - t \sum_{\langle i,j\rangle} (A^\dagger_{\mathbf{R}_i} B_{\mathbf{R}_j} + \text{H.c.}), \tag{2}$$

where the notation $\langle i, j\rangle$ indicates sums over all sites j and their nearest neighbors i. In graphene the A sites are identical to the B sites modulo a π rotation, so the energies $\mathcal{E}_A = \mathcal{E}_B$. Following Semenoff [4], we allow for different site energies ($\mathcal{E}_A \neq \mathcal{E}_B$), as in hexagonal boron nitride, and take the graphene limit where appropriate.

Introducing the Fourier transform of the operators $A_{\mathbf{R}_i} = \sum_j A_{\mathbf{Q}_j} \exp(i\mathbf{R}_i \cdot \mathbf{Q}_j)/\sqrt{N}$, where the $\mathbf{Q}_j = \frac{m}{N_1}\mathbf{b}_1 + \frac{n}{N_2}\mathbf{b}_2$ are the $N = N_1 N_2$ wave vectors in the first Brillouin zone, puts the Hamiltonian (2) in the form

$$H = \sum_j (A^\dagger_{\mathbf{Q}_j} \;\; B^\dagger_{\mathbf{Q}_j}) \mathcal{H} \begin{pmatrix} A_{\mathbf{Q}_j} \\ B_{\mathbf{Q}_j} \end{pmatrix}, \tag{3}$$

where we have used the closure relation $\sum_j e^{i\mathbf{R}_j \cdot (\mathbf{Q} - \mathbf{Q}')} = N\delta_{\mathbf{Q},\mathbf{Q}'}$, and defined the single particle Hamiltonian

$$\mathcal{H} = -t \begin{pmatrix} -\Delta/t & 1 + e^{-i\mathbf{Q}\cdot\mathbf{a}_1} + e^{-i\mathbf{Q}\cdot\mathbf{a}_2} \\ 1 + e^{i\mathbf{Q}\cdot\mathbf{a}_1} + e^{i\mathbf{Q}\cdot\mathbf{a}_2} & \Delta/t \end{pmatrix}. \tag{4}$$

Here the energy difference Δ is defined by $\Delta \equiv (\mathcal{E}_A - \mathcal{E}_B)/2$, and the energy origin is chosen such that $(\mathcal{E}_A + \mathcal{E}_B)/2 = 0$. Graphene has two atoms per unit cell, each of which donates one electron to the valence band, so in the lowest approximation the first Brillouin zone is exactly filled. Thus the Fermi energy is zero here.

The off-diagonal matrix elements of the $\mathcal{H}$ matrix (4) vanish at the corners $\mathbf{Q} = \mathbf{K}$ of the Brillouin zone (see Fig. 1), which in the graphene case $\mathcal{E}_A = \mathcal{E}_B$ leads to the famous degeneracy at these "Dirac points": $\mathbf{K}^\kappa = \kappa\frac{2\mathbf{b}_2 + \mathbf{b}_1}{3} + m\mathbf{b}_1 + n\mathbf{b}_2$ [12]. Here $\kappa = \pm 1$ is the "valley" index that distinguishes the two inequivalent types of $\mathbf{K}$ points. To see the structure of low-energy excitations near the Dirac points we define $\mathbf{k} = \mathbf{Q} - \mathbf{K}$ and restrict our analysis to the case where $\mathbf{k} \cdot \mathbf{a}_i$ is small. Recalling $\mathbf{a}_i \cdot \mathbf{b}_j = 2\pi\delta_{ij}$, to lowest order

$$\mathcal{H} = \begin{pmatrix} \Delta & \sqrt{3}ta\mathbf{k}(\kappa\hat{\mathbf{a}}_d - i\hat{\mathbf{a}}_s)/2 \\ \sqrt{3}ta\mathbf{k}(\kappa\hat{\mathbf{a}}_d + i\hat{\mathbf{a}}_s)/2 & -\Delta \end{pmatrix}, \tag{5}$$

where we have defined difference and sum unit vectors $\hat{\mathbf{a}}_d = (\mathbf{a}_1 - \mathbf{a}_2)/a$ and $\hat{\mathbf{a}}_s = (\mathbf{a}_1 + \mathbf{a}_2)/\sqrt{3}a$. (A third vector $\hat{\mathbf{a}}_n \equiv \hat{\mathbf{a}}_d \times \hat{\mathbf{a}}_s$ normal to the plane will also prove useful.) The Hamiltonian (5) is a rotational invariant, depending only on scalars and the scalar products of 3D vectors. As shown in Fig. 1, the eigenvalues of $\mathcal{H}$ are independent of the direction of $\mathbf{k}$ near $\mathbf{K}$, which is to say that the Hamiltonian is effectively isotropic in the plane—the lattice has disappeared.

The analysis leading to (5) has been entirely in terms of the basis vectors of the direct and reciprocal lattices of the honeycomb structure, and is independent of any choice of orientation for a 3D Cartesian coordinate system. The predictions of the theory are independent of this choice. Two particular orientations put $\mathcal{H}$ in familiar and suggestive forms. Choosing the coordinate orientations labeled "D" and "P" in Fig. 1, defining the Fermi velocity $v_F = \sqrt{3}at/2\hbar$, and writing the momentum $\mathbf{p} = \hbar\mathbf{k}$ gives

$$\mathcal{H}_D = v_F(\kappa\sigma_x p_y - \sigma_y p_x) + \sigma_z\Delta \quad \text{and} \tag{6a}$$

$$\mathcal{H}_P = v_F(\kappa\sigma_x p_x + \sigma_y p_y) + \sigma_z\Delta, \tag{6b}$$

where the σ_j are the usual Pauli matrices. The matrix $\mathcal{H}_D$ (6a) illustrates the connection between the graphene Hamiltonian and the Dirac equation. In 3 + 1 dimensions the Dirac Hamiltonian is $H = c\gamma^0(\boldsymbol{\gamma}\cdot\mathbf{p} + mc)$, with 4×4 matrices $\gamma^\mu = (\gamma^0, \boldsymbol{\gamma})$. In 2 + 1 dimensions the necessary anticommutation relations $\{\gamma^\mu, \gamma^\nu\} = 2g^{\mu\nu} = 2 \times \text{diag}(1, -1, -1)$ can be satisfied with a 2×2 representation such as $\gamma^\mu = (\gamma^0, \vec{\gamma}) = (\sigma_z, i\sigma_x, i\kappa\sigma_y)$. With this definition the Hamiltonian matrix (6a) becomes $\mathcal{H} = v_F\gamma^0(\vec{\gamma}\cdot\vec{p} + m'v_F)$, with an effective mass m' defined by $\Delta = m'v_F^2$. (We designate the first two components of a 3D vector with an arrow, e.g., $\mathbf{p} = p_x\hat{\mathbf{x}} + p_y\hat{\mathbf{y}} + p_z\hat{\mathbf{z}} = \vec{p} + p_z\hat{\mathbf{z}}$.) Thus this hopping model gives low-energy electronic excitations that obey a 2 + 1 dimensional Dirac equation, with the Fermi velocity v_F playing the usual role of the speed of light c.

With the P coordinate orientation graphene's Hamiltonian matrix has the convenient abbreviation $\mathcal{H} = v_F \vec{\sigma} \cdot \vec{p}$ near $\mathbf{K}^+$. Sometimes this is written $\mathcal{H} = v_F \boldsymbol{\sigma} \cdot \mathbf{p}$, which can give the impression that either σ_z or p_z is strictly zero. In fact, both $\boldsymbol{\sigma}$ and $\mathbf{p}$ have three nonzero components; it just happens that σ_z and p_z do not appear in the graphene $\mathcal{H}$. While any state confined to the sheet must have an expectation value $\langle p_z \rangle = 0$, because the electrons are localized in z the characteristic magnitude of p_z is $\hbar/a_z$, where a_z is a length scale measuring the z extent of the $2P_z$ orbitals of the expansion (1). Taking $p_z = 0$ is just as improper for an electron in a honeycomb lattice as it is for an electron in an atomic Coulomb potential. The case of σ_z will be taken up below.

It is not obvious whether $\boldsymbol{\sigma}$, which indexes the "pseudospin" arising from the AB sublattice degeneracy, corresponds to a real angular momentum [3,13]. It might describe a merely analogous two-state system, borrowing the same $SU(2)$ algebra like the isospin symmetry connecting the proton and neutron. Comparison with the $3 + 1$ dimensional Dirac equation makes this second option look likely. The 4×4 Dirac matrices give each state two qubits, one each for particle or antiparticle and spin-up or spin-down values. Since the pseudospin labels the band index β [see Eq. (9) below] and the 2D Dirac matrices are only 2×2, it would seem that the one qubit available is engaged.

Surprisingly, this one qubit covers both variables. The pseudospin is related to a real angular momentum, as can be discovered by calculating the commutator of the Hamiltonian with the orbital angular momentum $\mathbf{L} = \mathbf{r} \times \mathbf{p}$,

$$[\mathcal{H}_P, \mathbf{L}] = -i\hbar v_F \begin{pmatrix} \sigma_y p_z \\ -\kappa \sigma_x p_z \\ \kappa \sigma_x p_y - \sigma_y p_x \end{pmatrix}. \tag{7}$$

That the Hamiltonian has rotational symmetry about the axis perpendicular to the plane and the commutator $[\mathcal{H}_P, L_z]$ is not zero together indicate that there is another angular momentum in the problem.

In coordinate-independent notation the honeycomb Hamiltonian (5) is

$$\mathcal{H} = \frac{2\kappa v_F}{\hbar} \mathbf{S} \cdot \mathbf{u}, \quad \text{where} \tag{8a}$$

$$\mathbf{S} \equiv \frac{\hbar}{2} (\sigma_x \hat{\mathbf{a}}_d + \kappa \sigma_y \hat{\mathbf{a}}_s + \kappa \sigma_z \hat{\mathbf{a}}_n), \quad \text{and} \tag{8b}$$

$$\mathbf{u} \equiv (\mathbf{p} \cdot \hat{\mathbf{a}}_d) \hat{\mathbf{a}}_d + (\mathbf{p} \cdot \hat{\mathbf{a}}_s) \hat{\mathbf{a}}_s + (\Delta / v_F) \hat{\mathbf{a}}_n. \tag{8c}$$

The operator $\mathbf{S}$ defined by (8b) we term "lattice spin" to distinguish it from both the dimensionless pseudospin and the usual electron spin. One can easily verify that $[\mathcal{H}, (\mathbf{L} + \mathbf{S}) \cdot \hat{\mathbf{a}}_n] = 0$ for any value of Δ. Thus neither the lattice spin nor the orbital angular momentum is separately a constant of the motion, but the projection of the total angular momentum $\mathbf{J} \equiv \mathbf{L} + \mathbf{S}$ onto the plane-normal axis (the z axis for P or D coordinates) is a conserved quantity. It is not possible to confuse $\mathbf{S}$ with an orbital angular momentum, as its eigenvalues have half-integer magnitude in units of $\hbar$.

Since earlier work asserts that the pseudospin is not associated with an angular momentum [3,13], it is worth exploring why we are led to a different result. In a strictly 2D system angular momentum is defined only in a limited sense. There is only one generator corresponding to (commuting) rotations about the direction normal to the plane [13], which is inconsistent with a $3 + 1$ dimensional spin. By confining the electrons, the graphene sheet produces an electronic Hamiltonian $\mathcal{H} \propto \mathbf{S} \cdot \mathbf{u}$ which lacks the full 3D rotational symmetry of the vacuum. However, the (scalar) Hamiltonian is invariant under rotations of the system relative to the three coordinate axes, and the generators of these rotations, i.e., the angular momentum operators, are still well defined. And unlike two-level systems that can be reduced to the spin-1/2 problem by analogy only, the honeycomb structure produces a spin variable specified in relation to a laboratory coordinate system. In other words, the direction of $\mathbf{u}$, like that of a magnetic field $\mathbf{B}$, can be related to "east," where no such relation appears in, say, the isospin problem. Since the operator $R(\mathbf{n}, \Phi) = \exp(-i\Phi \mathbf{S} \cdot \hat{\mathbf{n}}/\hbar)$ generates a rotation of the observable $\mathbf{S}$ by an angle Φ about the $\hat{\mathbf{n}} \equiv \mathbf{n}/|\mathbf{n}|$ axis, where $\hat{\mathbf{n}}$ is a direction in real space, $\mathbf{S}$ must be a real angular momentum [14].

The analogy between the vector $\mathbf{u}$ and a magnetic field $\mathbf{B}$ is helpful for understanding the close relationship between energy and angular momentum that follows from the $\boldsymbol{\sigma}$ operator's coverage of both qubits. We compare the time evolution operator $U = \exp(-i\mathcal{H}t/\hbar)$ with the rotation operator $R(\mathbf{u}, \Phi)$. For the honeycomb Hamiltonian (8a) these expressions are identical; time evolving the state is equivalent to rotating it about the $\hat{\mathbf{u}}$ axis at a rate $d\Phi/dt = (E_+ - E_-)/\hbar$. The energies E_β correspond to the two eigenvalues of the Hamiltonian $\mathcal{H}$,

$$E_\beta = \beta \sqrt{v_F^2 (p_x^2 + p_y^2) + m'^2 v_F^4}, \tag{9}$$

where we have defined the band index $\beta = \pm 1$. An equivalent relationship between time evolution and rotations appears when a magnetic dipole is placed in a magnetic field $\mathbf{B}$, where it is called Larmor precession. The time evolution of the lattice spin operator is given by [14]

$$\frac{d\mathbf{S}}{dt} = \frac{2\kappa v_F}{\hbar} \mathbf{u} \times \mathbf{S}, \tag{10}$$

which is exactly the equation of motion of a magnetic dipole in a magnetic field, with the substitution $2\kappa v_F \mathbf{u}/\hbar \rightarrow -\gamma \mathbf{B}$ (here γ is the gyromagnetic ratio). Thus the mixing between helicity eigenstates produced by a mass term in the $2 + 1$ dimensional Dirac Hamiltonian is formally identical to the mixing between

spin-up and spin-down states produced by perpendicular magnetic field $\mathbf{B}_\perp$. In the general case of $\mathbf{u}$ not parallel to $\mathbf{S}$, Eq. (10) shows that the components of $\mathbf{S}$ perpendicular and parallel to the plane interconvert as a function of time.

Relating pseudospin to angular momentum provides an intuitive explanation, the existence of which has long been suspected [15], for some properties of graphene and related materials [14]. For instance, in metallic nanotubes the backscattering of electrons is suppressed if the scattering potential has a range that is long compared to a lattice constant [15,16]. Since such a potential will treat A and B sites identically, it is a scalar with respect to the lattice spin, and thus cannot create the lattice spin flip required to reverse the electron motion. Conservation of pseudospin or lattice spin also provides a way to understand Klein tunneling in graphene [11], and emphasizes the equivalence between the condensed matter and particle physics systems.

As another example, interpreting the pseudospin as connected to a real angular momentum gives a satisfying picture of photon-mediated electron-hole pair production (or recombination) in graphene. In this process an electron with pseudospin parallel to its momentum transitions between the negative energy valence band and the positive energy conduction band, absorbing (or emitting) a photon and flipping its pseudospin [17,18]. Both bands are derived from atomic $2P_z$ orbitals, and the electron spin does not flip, so the usual sources do not contribute to the photon's angular momentum. A full description [19] of this process based on the Hamiltonian (6b) and the substitution $\mathbf{p} \rightarrow \mathbf{p} - q\mathbf{A}/c$ (with the quantized vector potential $\mathbf{A}$ describing the photon) shows that the photon's polarization couples the initial and final pseudospin states. As the photon's vector polarization is associated with its spin $\hbar$, the transition matrix element requires that the pseudospin be associated with an angular momentum $\hbar/2$.

Spin states have been previously associated with specific types of sites in a lattice within the ''staggered'' formulation of lattice quantum chromodynamics [20]. However, the hypercubic lattice chosen there is a convenient framework for discretizing the Dirac equation, not the basis of a more fundamental model from which the Dirac equation emerges naturally. The hypercubic lattice cannot be viewed as a discretized space through which particles move, since necessary phase tuning in the lattice Hamiltonian [20,21] ruins its hopping interpretation for $D > 1$. Furthermore, the number of sublattices must be fixed artificially using foreknowledge of the Dirac equation. These differences are not solely aesthetic; unlike the unphysical Hamiltonian contrived for the hypercubic lattice, the honeycomb Hamiltonian can be studied in optical lattices [22] and natural materials such as graphene [4,17,18].

By generating an internal quantum number that reflects an energy scale much larger than the host particle's mass [2], the graphene example invites connection to the intrinsic spin carried by the quarks and leptons. However, it is not obvious that a lattice can be found that naturally produces the $3 + 1$ dimensional Dirac equation [23,24], let alone the chiral properties of the full standard model [25,26]. Thus there are two possibilities, depending on whether these spins have related origins. Either intrinsic spin is also the low-energy signature of nontrivial quantized space, or lattice spin represents a second, experimentally accessible type of quantum mechanical angular momentum with no classical analogue.

*regan@physics.ucla.edu

[1] S. Tomonaga, *The Story of Spin* (University of Chicago Press, Chicago, 1997).
[2] K. Hagiwara, K. Hikasa, M. Tanabashi, and P. D. Group, Phys. Lett. B **667**, 1209 (2008).
[3] D. P. DiVincenzo and E. J. Mele, Phys. Rev. B **29**, 1685 (1984).
[4] G. W. Semenoff, Phys. Rev. Lett. **53**, 2449 (1984).
[5] P. R. Wallace, Phys. Rev. **71**, 622 (1947).
[6] S. Iijima, Nature (London) **354**, 56 (1991).
[7] K. S. Novoselov *et al.*, Science **306**, 666 (2004).
[8] R. Saito, G. Dresselhaus, and M. S. Dresselhaus, *Physical Properties of Carbon Nanotubes* (Imperial College Press, London, 1998).
[9] A. H. C. Neto *et al.*, Rev. Mod. Phys. **81**, 109 (2009).
[10] M. I. Katsnelson and K. S. Novoselov, Solid State Commun. **143**, 3 (2007).
[11] M. I. Katsnelson, K. S. Novoselov, and A. K. Geim, Nature Phys. **2**, 620 (2006).
[12] C. Bena and G. Montambaux, New J. Phys. **11**, 095003 (2009).
[13] V. P. Gusynin, S. G. Sharapov, and J. Carbotte, Int. J. Mod. Phys. B **21**, 4611 (2007).
[14] See supplemental material at http://link.aps.org/supplemental/10.1103/PhysRevLett.106.116803 for a proof and further discussion.
[15] T. Ando and T. Nakanishi, J. Phys. Soc. Jpn. **67**, 1704 (1998).
[16] P. L. McEuen *et al.*, Phys. Rev. Lett. **83**, 5098 (1999).
[17] A. B. Kuzmenko *et al.*, Phys. Rev. Lett. **100**, 117401 (2008).
[18] R. R. Nair *et al.*, Science **320**, 1308 (2008).
[19] M. Mecklenburg, J. Woo, and B. C. Regan, Phys. Rev. B **81**, 245401 (2010).
[20] L. Susskind, Phys. Rev. D **16**, 3031 (1977).
[21] A. Zee, in *M. A. B. Beg Memorial Volume*, edited by A. Ali and P. Hoodbhoy (World Scientific, Singapore, River Edge, NJ, 1991), pp. 129–140.
[22] P. Soltan-Panahi *et al.*, arXiv:1005.1276v1 [Nature Phys. (in press)].
[23] M. Creutz, J. High Energy Phys. 04 (2008) 017.
[24] P. F. Bedaque *et al.*, Phys. Rev. D **78**, 017502 (2008).
[25] H. B. Nielsen and M. Ninomiya, Nucl. Phys. **B185**, 20 (1981).
[26] S. Chandrasekharan and U. J. Wiese, Prog. Part. Nucl. Phys. **53**, 373 (2004).